CaMKII binds both substrates and effectors at the active site

Can Özden[1,2], Roman Sloutsky[1], Nicholas Santos[1], Emily Agnello[1], Christl Gaubitz[4], Emily Lapinskas[1], Joshua Foster[2], Edward A. Esposito[3], Brian A. Kelch[4], Scott C. Garman[1], Yasunori Hayashi[5], Margaret M. Stratton[1]†

[1]Department of Biochemistry and Molecular Biology, University of Massachusetts, Amherst, MA 01003, USA. [2]Molecular and Cellular Biology Graduate Program, University of Massachusetts, Amherst, MA 01003, USA. [3]Malvern Panalytical, [4]Department of Biochemistry and Molecular Pharmacology, University of Massachusetts, Worcester, MA 01605, USA. [5]Department of Pharmacology, Kyoto University Graduate School of Medicine, Kyoto, Japan.

† Corresponding author. Email: mstratton@umass.edu (M.M.S.)

ABSTRACT

Ca^{2+}/calmodulin dependent protein kinase II (CaMKII) is a signaling protein that is required for long-term memory formation. Ca^{2+}/CaM activates CaMKII by binding to its regulatory segment, thereby freeing the substrate binding pocket. One exceptional feature of this kinase is that interaction with specific binding partners persistently activate CaMKII after the Ca^{2+} stimulus dissipates. The molecular details of this phenomenon are unclear. Despite having a large variety of interaction partners, the specificity of CaMKII has not been structurally well-characterized. We solved X-ray crystal structures of the CaMKII kinase domain bound to four different effectors that modulate CaMKII activity. We show that all four partners use similar interactions to bind across the substrate binding pocket of the CaMKII active site. We generated a sequence alignment based on our structural observations, which revealed conserved interactions. The structures presented here shed much-needed light on CaMKII interactions. These observations will be crucial in guiding further biological experiments.

INTRODUCTION

Ca^{2+}/calmodulin-dependent protein kinase II (CaMKII) is a central signaling protein that controls various cellular functions such as synaptic plasticity, cytoskeletal regulation, cell growth and division, gene transcription and ion channel modulation [1]. CaMKII biology has been an active focus of research especially because of its crucial role in long-term potentiation (LTP), which is the basis for long-term memory [2, 3]. CaMKII is highly abundant in the forebrain postsynaptic density (PSD) fraction, where it makes up to 2% of total protein [4]. CaMKII is a multisubunit complex made up of 12-14 subunits, which is oligomerized by the hub domain (**Fig. 1a**). Each CaMKII subunit contains a Ser/Thr kinase domain, autoinhibitory/regulatory segment, variable linker region, and a hub domain (**Fig. 1b**).

CaMKII interacts with and phosphorylates dozens of synaptic proteins also known to play key roles in LTP (**Fig. 1c**). Intriguingly, some binding partners, or effectors, are substrates, some are inhibitors, and some have been shown to persistently activate CaMKII. The structural details explaining these disparities remain elusive. To begin untangling this, we first need to understand the specificity driving these interactions. We chose to structurally characterize four peptides from interactors that sample multiple functional outputs: AMPA-type glutamate receptor is a substrate, NMDA-type glutamate receptor is a substrate and activator, Tiam1 is an activator, and Densin-180 is an inhibitor [5-7].

Ca^{2+}/calmodulin (Ca^{2+}/CaM) activates CaMKII by binding to the regulatory segment and thereby freeing the substrate binding pocket. This well-understood mechanism triggers autophosphorylation of T286 within the autoinhibitory segment, which renders CaMKII constitutively active. CaMKII is also activated by another mechanism that invokes two binding sites [8-11], for which we lack a clear mechanism. There are two binding partners (NMDA receptor and Tiam1) that have been shown to be activators of CaMKII after the Ca^{2+} stimulus dissipates [9-11]. The GluN2B subunit of the NMDA receptor is a known substrate of CaMKII, and to this point, the best studied CaMKII activator. Ca^{2+}/CaM-activated CaMKII has been shown to form a persistent complex with GluN2B, which locks CaMKII in an active conformation, as long as binding persists. To date, persistent binding of CaMKII to GluN2B and resultant persistent activation has been explained by a hypothetical sequential transition model [10] . In this model, GluN2B first binds to CaMKII close to the active site (termed S-site), presenting Ser 1303 for phosphorylation. Next, GluN2B changes its position away from the active site and toward the base of CaMKII C-lobe (termed T-site), while freeing the S-site to bind other substrates. Although this model has been widely accepted in the field, there has been no structural confirmation.

In addition to structurally interrogating the GluN2B interaction, we are studying Tiam1, Densin-180, and AMPA receptor, all of which play key roles in LTP and interact with CaMKII. Tiam1 is a Rac guanine-nucleotide exchange factor (RacGEF), and also a CaMKII substrate. However, the Tiam1 peptide we interrogate here is a known activator, as mentioned above, and a pseudosubstrate (Ala at the phosphorylation site) [11]. Densin-180 (LRRC7) is a postsynaptic scaffolding protein and the peptide we use herein is a known inhibitor of CaMKII (Ile at the phosphorylation site) [12, 13]. Finally, the AMPA receptor subunit GluA1 is a CaMKII substrate but not a known activator. GluA1 phosphorylation has been shown to be important for synaptic plasticity [14-16]. There are two existing crystal structures of the CaMKII kinase domain bound to different effectors. One is CaMKIINtide, a peptide inhibitor of CaMKII derived from CaMKIIN1 [17] and the second is the *Drosophila* EAG potassium channel (*d*EAG) carboxyl tail, which is a known CaMKII substrate [18].

In the current study, we solved new co-crystal structures of the CaMKII kinase domain bound to peptides from GluN2B, Tiam1, Densin-180, and GluA1. Using these structures as starting points, we performed molecular dynamics (MD) simulations of the kinase domain in complex with GluN2B, Tiam1, and CaMKIIN1. These structures show the peptides bound in the same binding site on the kinase domain as previously observed with *d*EAG and CaMKIINtide. Combining this structural information with observations obtained from MD simulations has allowed us to clarify important interactions that drive binding.

RESULTS

CaMKII kinase domain interactions with four different binding partners

We used a fluorescence polarization (FP) assay to measure binding of CaMKII kinase domain to peptides of five interactors: GluN2B (1289-1310), GluA1 (818-837), Densin-180 (797-818), Tiam1 (1541-1559), and CaMKIINtide (37-58). Four out of five tested peptides bind with similar affinities (K_d values 1.3 - 4.5 μM) (GluN2B K_d = 1.3 μM, CaMKIINtide K_d = 2.9 μM, Densin-180 K_d = 3.4 μM, and Tiam1 K_d = 4.5 μM) (**Fig. 2b**). The one exception was GluA1, which bound with a significantly lower affinity compared to the others (K_d = 95 μM) (**Fig. 2b**). For comparison, we include CaMKIINtide in these studies, as this is a known endogenous inhibitor of CaMKII [19-21]. Unless otherwise specified, crystallographic and fluorescence polarization (FP) experiments were conducted in the background of an inactivating CaMKII mutation (D135N). Herein, we will identify key interactions observed in the structures and simulations that mediate these interactions.

We solved crystal structures of the kinase domain of CaMKII bound to four peptides of known interactors (**Fig. 2, S1**). These include NMDA and AMPA receptor peptide substrates (GluN2B 1289-1310 and GluA1 818-837, respectively), Densin-180 (797-818) and Tiam1 (1541-1559). All four crystal structures have resolutions within the range of 1.8 - 2.7 Å (Table 1, 2). The overall fold of the kinase domain is similar in all structures with a range of Cα RMSD values from 0.583 to 1.611 Å.

We solved 9 structures of the CaMKII kinase domain bound to GluN2B peptide variants with different molecules bound in the active site. In four structures (physiologically irrelevant dimer in asymmetric unit), the D135N kinase domain is bound to the WT or phosphomimetic version of the GluN2B peptides (S1303D) with either ATP (PDB:6XBX) or methyl 6-O-(N-heptylcarbamoyl)-alpha-D-glucopyranoside (Hecameg), a mild detergent molecule, in the active site. Both ATP and Hecameg form hydrogen bonds with the backbone carboxy group of D90 and the backbone amino group of V92. We then solved 3 structures (monomers in asymmetric unit) of the D135N kinase domain bound to a phosphomimetic GluN2B peptide, with both ATP bound or empty active site. Finally, WT kinase domain was crystallized with the GluN2B peptide bound with either ADP bound (PDB:6XDU) or an empty active site (PDB:6XDL). In these structures, there was better resolution at the C-terminus of the peptide compared to previous structures.

All peptides bound similarly, interacting with the same surface on the kinase domain. We resolved 14-19 residues in each peptide (**Fig. 2a, S1**). GluN2B and Densin-180 bound in a completely extended conformation across the substrate binding pocket, whereas Tiam1 and GluA1 adopt short helical turns at the N-terminal end of the peptides, similar to what was previously observed in the CaMKIINtide structure [17]. Additionally, Densin-180 forms an intrachain electrostatic interaction between the -3 position arginine and upstream aspartate.

We performed MD simulations of the kinase domain in complex with extended versions of peptides from GluN2B (1263-1328, adding 32 N-terminal residues and 20 C-terminal residues) and Tiam1 (1513-1581, adding 28 N-terminal residues and 22 C-terminal residues) and the full-length CaMKIIN1 protein (adding 41 N-terminal residues and 22 C-terminal residues). Trajectories were run for 1.2 μs - 3.7 μs aggregate time for each complex. GluN2B and Tiam1 complexes were prepared for simulation from structures solved in this study: PDB:6XBX and PDB: 6XF0, respectively. For the CaMKIIN1 complex, we aligned a previously solved CaMKIINtide structure (PDB:3KL8 [17]) with the GluN2B structure via the kinase domain, and then deleted the kinase domain from the CaMKIINtide structure and the GluN2B peptide to create the merged system containing kinase/ATP/Mg^{2+} from the GluN2B structure with the CaMKIINtide peptide.

Sequence alignment of CaMKII binding partners based on high-resolution structures

So far, prediction of CaMKII interaction partners has been difficult due to conformational heterogeneity in CaMKII binding. Our structures reveal that several peptides have helical turns, which shift the register of conserved interactions (Tiam1, GluA1, and the previously observed CaMKIINtide). We now provide an updated sequence alignment based on our structural observations (**Fig. 2c**). The two peptides that are substrates (GluN2B and GluA1) have the phosphosite facing the ATP binding pocket, such that both peptides are docked at the active site, ready to be phosphorylated. Herein, we use numbering based on the prototypical GluN2B substrate with the phosphorylation site set to zero, irrespective of the actual number in each protein. The critical residues of the binding partner mediating this interaction are conserved at positions +1, -2, -3, -5, and -8 (**Fig. 2c**).

Hydrophobic residues mediate binding interactions

Hydrophobic interaction at the +1 position. It had been noted that a small hydrophobic residue is preferred at the +1 position [18, 22-25], which we also observe in our structures (**Fig. 2c**). Val and Ile at the +1 position bind to the hydrophobic groove across G175, whereas Tyr of GluN2B was too large to fit into this groove and, therefore, faces out. In MD simulations, extended peptides interact via two residues (+1 and +4 positions in NR2B and Tiam1, +1 and +2 in CaMKIINtide; **Fig. S2f-h**) with a hydrophobic patch formed by F173, P177, L185, and Y222. The +1 leucine and +4 isoleucine of Tiam1 pack with the four kinase residues into a conformation with high structural integrity, with RMSD of less than 2 Å (**Fig. S2f**). The interaction is more fluid for GluN2B and CaMKIIN1, but their respective residues remain in close proximity to the patch throughout the trajectory (**Fig S2g, h**).

Hydrophobic interaction mediated by a conserved leucine at the -5 position. All CaMKII interactors studied here have a conserved leucine residue at the -5 position to bind in a hydrophobic pocket on the kinase domain comprised of F98, I101, V102, and I205 (**Fig. 3, 4a**). In crystal structures the leucine residue is 3.3-4.5 Å away from the four hydrophobic residues, indicating tight interactions. In the CaMKIINtide structure, a turn motif is facilitated by two glycine residues, which orients the leucine into this pocket. This interaction also demonstrates high structural integrity throughout MD simulations of GluN2B, Tiam1, and CaMKIINtide, with RMSD below 2 Å (**Fig. 4b**).

Docking site mediated by W214. Both Densin-180 and CaMKIINtide pack against a tryptophan residue on the kinase domain (W214) in their respective crystal structures (**Fig. 4c**). In both structures, the sidechains of proline and isoleucine (highlighted blue in **Fig. 2c**) pack against this tryptophan. Additionally for Densin-180, the guanidino group of R808 at the -7 position hydrogen bonds with the backbone carbonyl group of W214 and the sidechain of Q224. In simulations of CaMKIIN, this interaction is persistent, with RMSD below 1.5 Å (**Fig. 4e**). In the trajectory of Tiam1 bound to the kinase domain, a leucine residue forms a persistent interaction with W214 (**Fig. 4c,e**, highlighted blue in **Fig. 2c**). In the Tiam1 crystal structure, the asymmetric unit is a dimer where this leucine is >13 Å from W214 in one monomer and not resolved in the other.

We measured peptide binding to a kinase domain mutant (W214A) using FP to determine the role of this tryptophan in docking. The W214A mutation completely abolished CaMKIINtide binding, whereas the effects on Densin-180, GluN2B, and Tiam1 binding were not as severe, decreasing the binding affinity 2- to 4-fold (**Fig. 4d, S2a-c**). Neither W214 nor W214A kinase binds GluA1 with any appreciable affinity.

Electrostatic interactions provide specificity

Ionic interactions mediated by the -2 position. Glutamine is commonly noted at the -2 position [18, 22-24]. However, it was previously unclear why this is favored due to insufficient structural data. All four of the peptides used in this study contain glutamine, allowing us to resolve important interactions mediated at this position. In crystal structures, we observe the amide oxygen of the glutamine sidechain forms a hydrogen bond with the backbone of G178, and the amino group interacts with the sidechain of Y179 of CaMKII. Additionally, the backbone carbonyl of glutamine interacts with sidechain of K137, and the backbone amino group of the -2 position interacts with E139, which has also been shown to be important for binding (**Fig. S3, S3j**) [10]. Of note, CaMKIINtide has a serine residue at the -2 position instead of glutamine (**Fig. 2c**). In this structure, the serine sidechain is flipped relative to the glutamine sidechains, which enables hydrogen bonding with E139 and K137 sidechains [17]. This observation is consistent with a previous study,

which showed that CaMKIINtide binding to CaMKII was reduced when this serine was mutated to alanine [26].

Conserved salt bridge close to the active site. The -3 position is a conserved basic residue, which interacts with conserved glutamate residues on the kinase domain, similar to previous observations [17, 27]. In the crystal structures, all interactors except for low-affinity binder GluA1, have a basic residue at the -3 position, which forms salt bridges with two glutamic acid residues (E96, E99) located on the αD helix of the kinase domain (**Fig. 5a**). The basic residues of interaction partners are positioned 2.4 – 4.2 Å between E96 and E99. In the Densin-180 and CaMKIINtide structures, the -3 residue is closer to E96, whereas in the Tiam1 structure, the -3 position is closer to E99. In the structures of GluN2B, the -3 position is either more closely associated with E96 (PDB:6XDL, WT kinase with empty active site; PDB:6XDU, WT kinase with ADP bound) or E99 (PDB:6XBP, D135N kinase with a detergent bound; PDB:6XBX, D135N kinase with ATP bound) (**Fig. S3a**). Additionally, in structures where ATP/Mg is also bound (GluN2B, Tiam1), the side chain of E96 interacts with the hydroxyl group of ribose in the ATP molecule (3.7 – 4.3 Å; **Fig. S3d**) [28]. This salt bridge is not formed in the GluA1 interaction, because there is a proline at the -3 position (**Fig. 2c**). In the GluA1 co-crystal structure, the sidechain of E96 is flipped away from the substrate compared to the other four structures where it is oriented toward the binding partner (**Fig. 5a**, inset). Additionally, the sidechain of E99 is not as well-resolved as it is in the other structures.

We hypothesized that the reason for GluA1's lower affinity compared to other interaction partners is due to the lack of this salt bridge. To test this, we created charge reversal mutations (E→K), and also E→Q mutations that maintain the possibility of hydrogen bonding, but not the electrostatic component. We directly compared binding affinities of GluN2B (which has a basic residue at the -3 position) to GluA1 which is lacking this interaction. Single E96K and E99K mutations were more disruptive to GluN2B binding (affinity decreased 7- and 5-fold, respectively) compared to GluA1 binding (affinity decreased <2-fold) (**Fig. 5b, c**). The double lysine mutation (E96/99K) significantly reduced the binding affinity for GluN2B peptide 52-fold (K_d = 68.7 μM), while the affinity for GluA1 was roughly the same. Overall, the E→Q mutations were less disruptive to binding. GluN2B binding to E96Q and E99Q was only marginally impaired (affinity decreased <2-fold), while the binding affinity of GluN2B for the double mutant E96/99Q was weakened by ~4-fold (K_d = 5 μM) (**Fig. S3b**). All glutamine mutants showed similar binding to GluA1 compared to WT, where the binding affinities were >77 μM (**Fig. S3c**). The double glutamine mutant (E96/99Q) expressed more poorly than WT, but the double lysine mutant (E96/99K) reduced the protein expression significantly, likely due to overall fold destabilization.

In MD simulations, the -3 residue also forms a persistent interaction with E139. The -3 arginine of GluN2B forms 2-4 ionic interactions nearly 100% of the time, mostly with E96 and E139 (**Fig S3g)**, while the lysine of Tiam1 forms 1-2 ionic interactions ~70% of the time, mostly with E139 (**Fig S3h**). There are no observed interactions between the ATP phosphate groups and the GluN2B and Tiam1 chains. The interactions observed in the CaMKIINtide trajectories were very different. The arginine at the -3 position mostly interacts with E139, minimally with E96, and not at all with E99 (**Fig. S3i**). The arginine residues at the 0 and -3 positions form very stable contacts with the ATP phosphates, which locks the ATP in an altered position (**Fig S3e, j**). This conformational change precludes the ATP adenosine from forming ionic interactions with the backbones of D90 and V92, as observed in the crystal structure. As a result, the ATP adenosine group exits the binding pocket in the CaMKIINtide trajectories (**Fig S3e**). In these trajectories, the serine at the -2 position of CaMKIINtide forms a hydrogen bond with E139 ~98% of the time (**Fig. S3j**), whereas in GluN2B and Tiam1 trajectories, the glutamine at the -2 position does not form stable interactions.

We performed FP measurements comparing binding of CaMKIINtide to the kinase domain with charge reversal mutations (E96K, E99K), with and without ATP (**Fig S3f**). In the absence of ATP, E96K and E99K both have a ~9-fold reduced binding affinity to CaMKIINtide. MD trajectories would predict that ATP binding is facilitated by the -3 arginine and E96, whereas E99 plays essentially no role. Consistent with this, ATP binding restored E99K binding similar to that of WT (D135N), whereas the affinity of E96K was still weakened.

Salt bridge at the base of the C-lobe. We observed a conserved basic residue at the -8 position (arginine or lysine) mediating a salt bridge with E236 on the kinase domain (**Fig. 2c, 3, 6a**). This likely has not been previously characterized because this position is quite far from the phosphorylation site (~30 Å), and substrate alignments have not been accurate enough to highlight the conservation at this position. We tested the effect of mutating E236 to lysine (E236K) on binding affinity. The E236K mutation completely abolished both Tiam1 and CaMKIINtide binding, whereas the effects on GluN2B, Densin-180, and GluA1 binding were more subtle (**Fig 6b, S4a, b**). For Densin-180, E236K binding affinity was reduced ~6-fold (K_d = 21 μM). For GluN2B, the E236K mutation did not entirely disrupt the interaction with the GluN2B peptide, but the K_d was weakened ~7-fold (K_d = 9 μM), which is consistent with previous studies [10]. We investigated whether peptide phosphorylation has an effect on binding affinity by measuring the affinity of D135N and D135N/E236K to the GluN2B peptide with a phosphomimetic substitution (S→D at position 0). There was very little effect on the phosphomimetic GluN2B binding to D135N (K_d = 2 μM), whereas affinity for the E236K mutant was reduced ~14-fold (K_d = 28 μM) (**Fig. 6c**).

We investigated the role of E236 in the MD trajectories, which revealed an additional interaction. In addition to interacting with the -8 position, E236 also forms a persistent H-bond with the hydroxyl group of Y210, thereby locking the Y210 side chain into a persistent interaction with W237 with very high structural integrity (RMSD <0.75 Å) (**Fig. S4c, g-i**). We performed simulations of GluN2B and Tiam1 complexes with an E236K mutation, which showed that the interaction between Y210 and W237 is disrupted by the loss of the H-bond with Y210 (**Fig. S4h, i**). The resulting movements of the Y210 side chain disrupt the W214 interaction with Tiam1, which may explain the loss of binding. In GluN2B, the interaction between Y210 and W237 is also disrupted, but the -8 arginine of GluN2B switches to a highly persistent interaction with D231.

Generalizing CaMKII binding partners

Finally, we mined the curated database of CaMKII phosphorylation sites (n=418) for consistencies with our updated alignment and found additional similarities (**Fig. 6e**, www.phosphosite.org). Hydrophobic residues (I, V, L, M, F) are found in +1, Q is found at -2, and R is overwhelmingly found at -3, but also at -2 and -4. Small hydrophobic residues (L, V, I or M) are found at -5 and -6. Generally, the minus direction disfavors P, D, and E. In contrast, acidic residues D and E are highly favored at +2. GluN2B has D at the +2 position, and we note an interaction with K56 in several structures, which was also observed in the *d*EAG-bound structure (PDB: 5H9B). In addition, S, which may serve as a second phosphorylation site, is strongly disfavored at nearly every position [18].

DISCUSSION

CaMKII has a broad range of substrates and interaction partners, yet the structural details driving these interactions have not been elucidated. We addressed this by solving co-crystal structures of four binding partners bound to the CaMKII kinase domain, which allowed us to highlight the interactions mediating binding. Like many other kinases, CaMKII prefers a basic residue at the -3 position on binding partners [29]. Our crystal structures, along with others [17, 28], show an electrostatic interaction between the -3 position and E96/E99. E96 is well-conserved across kinases and known to be important for ATP binding (**Fig. 6d, S3d**) [28]. E99 is not as well-

conserved, even across other CaM-kinases (**Fig. 6d**) [30]. Interestingly, the MD simulations also highlighted the role E139 plays in interactions with the -3 position (**Fig. S3g-j**). Previous studies have shown that mutations at E139 have a negative effect on AC-2 [27] and GluN2B [10] binding. Interestingly, our simulations show that E139 interacts with the -3 basic residue, consistent for all simulations in this study. The simulations also show the 0 and -3 positions (both arginine) of CaMKIIN1 strongly interact with ATP. Further efforts will interrogate the role of ATP coordination in CaMKIINtide inhibition.

Our mutagenesis data suggest that the decreased affinity of GluA1 to CaMKII is largely due to the absence of this salt bridge because charge reversal mutations do not significantly affect the affinity. The biological ramifications of this weak interaction between CaMKII and GluA1 will need to be investigated – where localization of CaMKII to this receptor by another factor or avidity effects of holoenzyme localization may be driving GluA1 phosphorylation [31]. A previous study showed reduced phosphorylation at S831 in neurons from a mouse harboring GluN2B mutations that block CaMKII binding, which would result in less CaMKII at the membrane perhaps leading to less interaction between CaMKII and GluA1 [32]. Moreover, our observation might explain the molecular basis of a recent study that reported lower levels of S831 phosphorylation in the hippocampus, which is contrary to previous data showing high levels of phosphorylation at this site [33, 34].

In CaMKII activation, the αD helix reorients outward, exposing a hydrophobic pocket for substrate binding, which we observed in all our structures. Kuriyan and colleagues first identified this hydrophobic pocket as 'docking site B', which is comprised of residues F98, I101, V102, and I205 [17]. The phenylalanine (F98) and isoleucine (I205) have been reported as potentially playing different roles in binding interactions, previously termed S- and T-sites, respectively [10, 27]. However, our data show that these residues comprise the same binding pocket, and are therefore not separate sites (**Fig. 3, 4a**). Highlighting the importance of this hydrophobic interaction, an F98 mutation has been shown to cause intellectual disability [35]. This hydrophobic pocket is highly conserved across CaM-kinases, but not other kinases (**Fig. 6d**). If we compare the structure of the kinase domain with an empty substrate binding site (PDB:6VZK) to structures of the kinase domain bound to a substrate, it is clear that F98 and V102 undergo a conformational change in the bound state to form a pocket (**Fig. S2d**). This indicates that these hydrophobic residues shift to accommodate substrate binding, which is likely a large contribution to an observed gain in kinase domain stability upon GluN2B binding (**Fig. S2e**), similar to what we have previously observed with regulatory segment binding, which is mediated by L290 in the regulatory segment [36]. All effectors studied here have a leucine at the -5 position. However, other binding partners also have small hydrophobic residues such as methionine (CaMKII regulatory segment) and isoleucine (phospholamban).

Although both CaMKIINtide and Densin-180 structures showed an interaction with W214, mutation at this site (W214A) abolished CaMKIINtide binding completely while only having a marginal effect on Densin-180 binding. Upon close examination, CaMKIINtide docking onto W214 is likely to stabilize its helical motif, which properly orients the -5 leucine into the hydrophobic pocket. When W214 is mutated, this interaction is disrupted and the leucine interaction is unlikely to be maintained in CaMKIINtide, completely disrupting binding. Densin-180 does not have a helical motif, which may explain why the W214A mutant does not have a drastic effect. A role for W214 was also proposed as a result of MD simulations between CaMKII and Coenzyme A [37]. Our MD trajectories of Tiam1 revealed that a leucine docks onto W214, which we did not observe in the crystal structure. Altogether, these data suggest that W214 may serve as a docking site for some CaMKII interaction partners, but not all, providing specificity.

Our simulations show persistent hydrophobic interactions between residues at the +1 and +2/+4 peptide positions and a surface hydrophobic patch comprised of F173, P177, L185, and Y222, consistent with a known preference for hydrophobic residues at the +1 position. Despite their persistence, these interactions do not have the same degree of peptide residue burial or, for GluN2B and CaMKIIN1, nearly the same degree of structural stability as the -5 hydrophobic interaction, and do not make a substantial contribution to binding affinity [11]. However, with the primary driver of binding located at the -5 peptide position, these + side interactions may serve an important role in maintaining the 0 position residue sufficiently proximal to the ATP binding pocket to facilitate phosphorylation, or prevent another substrate from being phosphorylated. This may be particularly important for Tiam1, which has a comparatively weak electrostatic interaction via the -3 lysine, but a comparatively strong +1 hydrophobic interaction.

In all crystal structures, we observed a salt bridge at E236 mediated by a basic residue at the -8 position. In the crystal structure solved with the fly kinase domain bound to a *d*EAG peptide, there is a glutamine residue interacting with E236 [18]. The effect of mutation at this site (E236K) had previously been tested on GluN2B binding, which did not show a significant change [10]. In the trajectory of E236K:GluN2B, the -8 arginine switches to interacting with D231, suggesting that this interaction may compensate for the E236K mutation. E236K is also unable to form the H-bond with Y210, making the tyrosine side chain more mobile in MD simulations, and disrupting the interaction between Tiam1 and W214. The interaction between CaMKIINtide and W214 is also likely to be disrupted by the E236K mutation. Consistent with this, our E236 mutagenesis studies showed varying effects, where CaMKIINtide and Tiam1 were most disrupted. Previous studies mutated Y210 without any significant loss of interaction with GluN2B and voltage-gated L-type Ca^{2+} channels [10, 38]. More work needs to be done to determine whether this electrostatic interaction provides some specificity, which could be exploited in biological experiments.

There is mounting evidence that specific interactions facilitate CaMKII activity against other substrates even in the absence of Ca^{2+}/CaM, yet there is not a clear molecular explanation for this. Further structural and biophysical analyses will be necessary to elucidate these binding partners, including GluN2B and Tiam1, can act as CaMKII activators while masking the entire substrate binding pocket (corresponding to both S- and T-sites). For these experiments, it will be important to consider how interactions may affect adjacent kinases within a holoenzyme complex. The crystal structures presented here provide clarity on the interactions between CaMKII and its binding partners, which will be crucial in guiding biological experiments to assess the downstream effects of specific interactions. These observations will be crucial in guiding further experiments, which will necessarily invoke the complexities of the CaMKII holoenzyme structure.

METHODS

Cloning

All CaMKIIα variants were expressed with an N-terminal His-SUMO tag in a pET vector. All point mutations were created using site-directed mutagenesis.

Protein Expression and Purification

WT CaMKIIα kinase domain (residues 7-274) was co-expressed with λ phosphatase in *E. coli* BL21(DE3). Inactive constructs (D135N) were expressed without λ phosphatase. The cells were induced at 18 °C with 1 mM Isopropyl β- d-1-thiogalactopyranoside (IPTG) and grown overnight. Following to ~16 hours incubation, cell pellets were resuspended in Buffer A (25 mM Tris, pH 8.5, 150 mM KCl, 40 mM imidazole, 10% glycerol) and commercially available protease inhibitors (0.5 mM Benzamidine, 0.2 mM AEBSF, 0.1 mg/mL trypsin inhibitor, 0.005 mM Leupeptin, 1 μg/mL Pepstatin), 1 μg/mL DNAse/50 mM $MgCl_2$ were added, then lysed. All

following purification steps were performed using an ÄKTA pure chromatography system at 4 °C. Filtered cell lysate was loaded onto a 5 mL His Trap FF NiNTA Sepharose column (GE), and eluted with 50% Buffer B (25 mM Tris-HCl pH 8.5, 150 mM KCl, 1 M imidazole, 10% glycerol). The protein was desalted from excess imidazole using a HiPrep 26/10 Desalting column using Buffer C (25 mM Tris-HCl pH 8.5, 40 mM KCl, 40 mM imidazole, 2 mM TCEP, 10% glycerol). His SUMO tags were cleaved with Ulp1 protease overnight at 4 °C. Cleaved His SUMO tags were separated by a subtractive NiNTA step prior to an anion exchange step. Proteins were eluted from HiTrap Q-FF with a KCl gradient. Eluted proteins were concentrated and further purified in gel filtration buffer (25 mM Tris-HCl pH 8.0, 150 mM KCl, 1 mM TCEP, 10% glycerol) using Superdex 75 10/300 GL size exclusion column. Fractions (>95% purity) were pooled, concentrated, aliquoted and flash frozen in liquid nitrogen, and stored at -80 °C until needed.

Peptide synthesis

Peptides used for co-crystallization were synthesized and amidated at the C-terminus (Genscript, RIKEN Research Resource Center). Peptides used for fluorescence polarization assays were synthesized with an additional N-terminal 5-FAM.

Full length peptide sequences are as follows:
Human GLUA1 (residues 818-837): SKRMKGFCLIPQQSINEAIR [Numbering for GluA1 is for mature peptide, excluding 18 amino acid long signal peptide, following convention in the field.]
Human GluN2B (residues 1289-1310): KAQKKNRNKLRRQHSYDTFVDL
Human GluN2B(S1303D) (residues 1289-1310): KAQKKNRNKLRRQHDYDTFVDL
Human Densin-180 (residues 797-818): SKSRSTSSHGRRPLIRQDRIVG
Mouse Tiam1 (residues 1541-1559): RTLDSHASRMTQLKKQAAL

Full length peptide sequences for fluorescence polarization assays are as follows:
Human GluA1 (residues 813-837): KSRSESKRMKGFCLIPQQSINEAIR
Human GluN2B (residues 1289-1310): KAQKKNRNKLRRQHSYDTFVDL
Human GluN2B(S1303D) (residues 1289-1310): KAQKKNRNKLRRQHDYDTFVDL
Human Densin-180 (797-818): SKSRSTSSHGRRPLIRQDRIVG
Human CaMK2N1 (residues 37-58): GAGQNKRPPKLGQIGRSKRVVI
Mouse Tiam1 (residues 1541-1559): RTLDSHASRMTQLKKQAAL

Crystallization and X-Ray Data Collection

Initial crystallization screening was done by the sitting vapor diffusion method at 4°C using commercially available screening kits. Initial hits were optimized by the hanging vapor diffusion method if needed. Conditions yielded the crystal formation were included in Table S1. The ligand-to-protein ratio was kept at 3:1 throughout the co-crystallization attempts. Diffraction data were collected from crystals flash-frozen in liquid nitrogen at a wavelength of 1.5418 Å using a Rigaku MicroMax-007 HF X-ray source, which was coupled to a Rigaku VariMax HF optic system (UMass Amherst). The X-ray data was collected at 100 K.

Data Processing and Structure Determination

Data sets were integrated, merged, and scaled using HKL-2000. The structures were solved by molecular replacement (MR) with Phaser using the coordinates of CaMKIIα kinase domain (PDB ID: 6VZK, 100% amino acid sequence identity) as a search model [39]. Peptides were built into electron density using Coot and refinement was performed with REFMAC5 [40, 41].

Binding assays

The fluorescent polarization experiment was executed by adding 10 µL of 120 nM fluorescein-labeled peptides (dissolved in 25 mM Tris pH 7.5, 150 mM KCl, 0.02% Tween, 0.02% Triton) to 10 µL of mutant CaMKII kinase domains at varying concentrations (25 mM Tris pH 7.5, 150 mM KCl, 1 mM TCEP, 10% glycerol) in Corning low volume 384-well black flat bottom 384-well plates. The concentration of ATP and $MgCl_2$ in peptide stock solution were adjusted to 500 µM and 10 Mm, respectively. The fluorescence polarization was measured using a Synergy H1 hybrid plate reader (Biotek) with a filter of 485/20 nm excitation and 528/20 nm emission. Data were fit using One site- Specific binding with Hill slope in GraphPad PRISM version 6.01 after subtracting the background value from individual values.

Molecular Dynamics simulations

Starting conformations were taken from co-crystal structures of CaMKIIα kinase domain in complex with peptides derived from GluN2B (PDB:6XBX) and Tiam1 (PDB:6XF0). For CaMKIIN1, Coot [41] was used to superimpose the structure of a peptide derived from rat CaMKIIN1 in complex with the kinase domain from *C. elegans* CaMKII (PDB:3KL8) with the structure of GluN2B in complex with the kinase domain of CaMKIIα bound to a Mg^{2+} ion and an ATP molecule (PDB:6XBX). The CaMKIIN1 peptide and the CaMKIIα kinase domain were then merged into a single structure. Crystallographically unresolved atoms were added, peptides were extended in both N-terminal and C-terminal directions, and E236K mutant versions of GluN2B and Tiam1 systems were created using PDBFixer, part of the OpenMM package [42].

All simulations were performed with Gromacs 2020.2 [43, 44] and the CHARMM36m force field [44]. Protein complexes were solvated with TIP3P water [45] in dodecahedral boxes that extended 1 nm past the protein in all dimensions. Na^+ ions were added in sufficient quantity to charge neutralize each system. Systems were energy-minimized by steepest descent for 50,000 steps using a 0.01 nm step size until the maximum force exerted on any atom fell below 1000 kJ/mol/nm. Solvent was equilibrated for 1 ns at constant temperature and volume (NVT ensemble) and another 2 ns at constant temperature and pressure (NPT ensemble) with a positional restraint applied to protein heavy atoms. Periodic boundary conditions were used in all dimensions, bonds were constrained with the LINCS algorithm [46], virtual sites (v-sites) were used to remove the fastest degrees of freedom to facilitate a 4 fs time step [47], particle mesh Ewald (PME) was used to treat electrostatic interactions [48], the v-rescale thermostat [49] with a 0.1 ps coupling time constant was used to maintain the temperature at 300 K, and a cut-off distance of 1.2 nm for neighbor list, Coulomb interactions, and Van der Waals interactions was used throughout system preparation and production simulations. The Parrinello–Rahman barostat [50] with a 2 ps coupling time constant was used used to maintain a pressure of 1 bar during NPT equilibration and production simulations. V-site parameters for ATP were determined using MkVsites [51].

One production simulation was performed for each of the wild type kinase:GluN2B and wild type kinase:Tiam1 complexes, producing trajectories of 2.19 µs and 2.05 µs, respectively. Two independent simulations were performed for each of wild type kinase:CaMKIIN1 and E236K kinase:GluN2B complexes. The CaMKIIN1 trajectories were 0.46 µs and 1.84 µs in length, for an aggregate of 2.3 µs. The GluN2B trajectories were 0.68 µs and 0.57 µs in length, for an aggregate of 1.25 µs. Four independent simulations were performed for the E236K kinase:Tiam1 complex, producing trajectories of 1.66 µs, 1.23 µs, 1.02 µs, and 0.77 µs, for an aggregate of 4.68 µs. Trajectories were analyzed using MDTraj [52].

Data availability

Atomic structures have been deposited in the PDB, listed in the table below.

Table of PDB codes and descriptions.

6X5G	Inactive kinase in complex with Densin-180
6X5Q	Inactive kinase in complex with GluA1
6X8V	Inactive kinase in complex with Tiam1
6XF0	Inactive kinase in complex with Tiam1 and ATP
6XBP	Inactive kinase in complex with GluN2B and Hecameg
6XBX	Inactive kinase in complex with GluN2B and ATP
6XDL	Active kinase in complex with GluN2B
6XDU	Active kinase in complex with GluN2B and ADP
7KL0	Inactive kinase in complex with phosphomimetic GluN2B and Hecameg
7KL1	Inactive kinase in complex with phosphomimetic GluN2B and ATP
7KL4	Inactive kinase in complex with phosphomimetic GluN2B
6XOE	Inactive kinase in complex with phosphomimetic GluN2B and ATP
7KL2	Inactive kinase in complex with phosphomimetic GluN2B

ACKNOWLEDGMENTS

We thank Roger Colbran for helpful discussions. This work was supported by start-up funds from UMass Amherst (M.S.), SPIRITS 2019 of Kyoto University, Grant-in-Aid for Scientific Research 18H04733, and 18H05434 from the MEXT, Japan and HFSP Research Grant (RGP0020/2019) (Y.H.).

Conflict of interest: YH received research funds from Fujitsu Laboratories and Dwango.

Author Contributions

C.Ö. solved all crystal structures and performed all FP measurements. N.S., E.A., C.G., E.L., J.F. and E.A.E. also assisted with experiments under supervision of B.A.K., S.C.G., Y.H. and M.M.S. R.S. performed molecular dynamics. C.Ö., R.S., Y.H., B.A.K., and M.M.S. wrote and edited the manuscript.

539 **FIGURES**
540

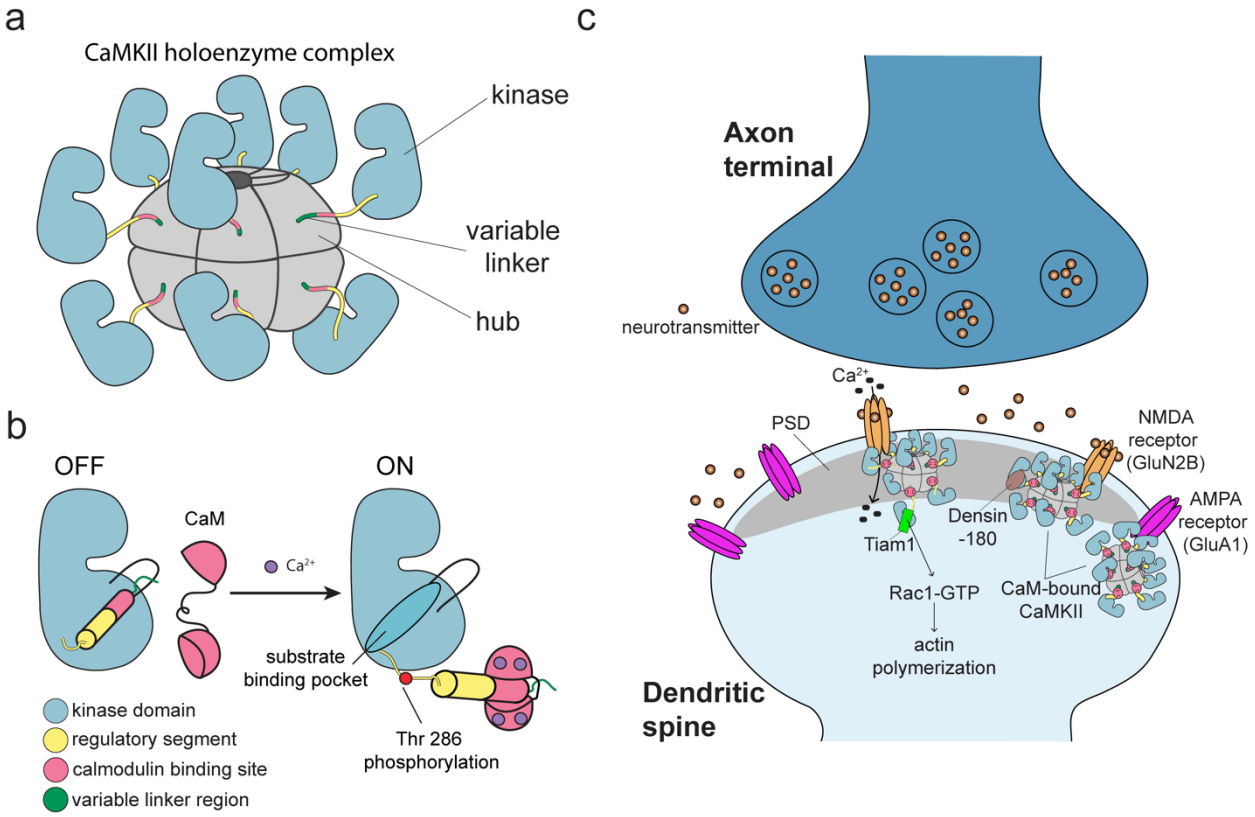

541
542
543 **Figure 1. CaMKII architecture and the interaction partners in excitatory synapses**
544 (a) The architecture of a dodecameric CaMKII holoenzyme. (b) Ca^{2+}/CaM binding activates
545 CaMKII by competitively binding the regulatory segment thereby freeing the substrate binding
546 pocket. Active CaMKII autophosphorylates at Thr 286. (c) CaMKII interactions at the excitatory
547 postsynaptic structure, mostly in the post synaptic density (PSD).
548
549

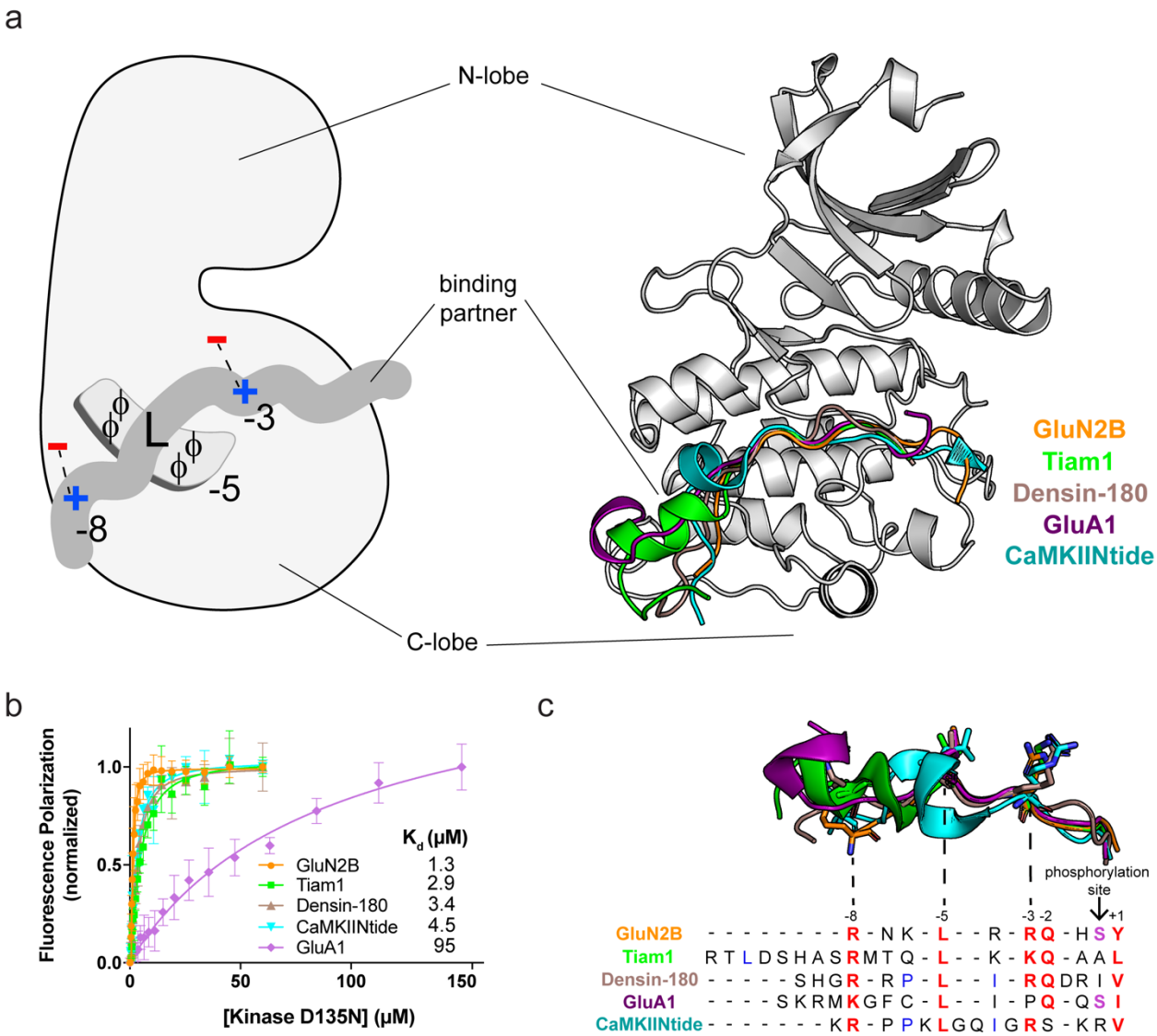

Figure 2. CaMKII kinase domain interactions with the binding partners. (a) Left: Schematic diagram of the interactions with binding partners. Phi symbol indicates hydrophobic residues. Green symbols indicate those identified from molecular dynamics simulations. Right: overlay of five cocrystal structures, peptides shown as cartoon in corresponding colors in (a). (b) Binding measurements for GluN2B, Tiam1, Densin-180, CaMKIINtide, and GluA1 using fluorescence polarization. (c) The sequence alignment of CaMKII binding partners. Aligned peptide structures are above. Conserved residues highlighted in red. Phosphosite residues on substrates are highlighted in purple. Residues involved in a docking event with W214 are highlighted in blue.

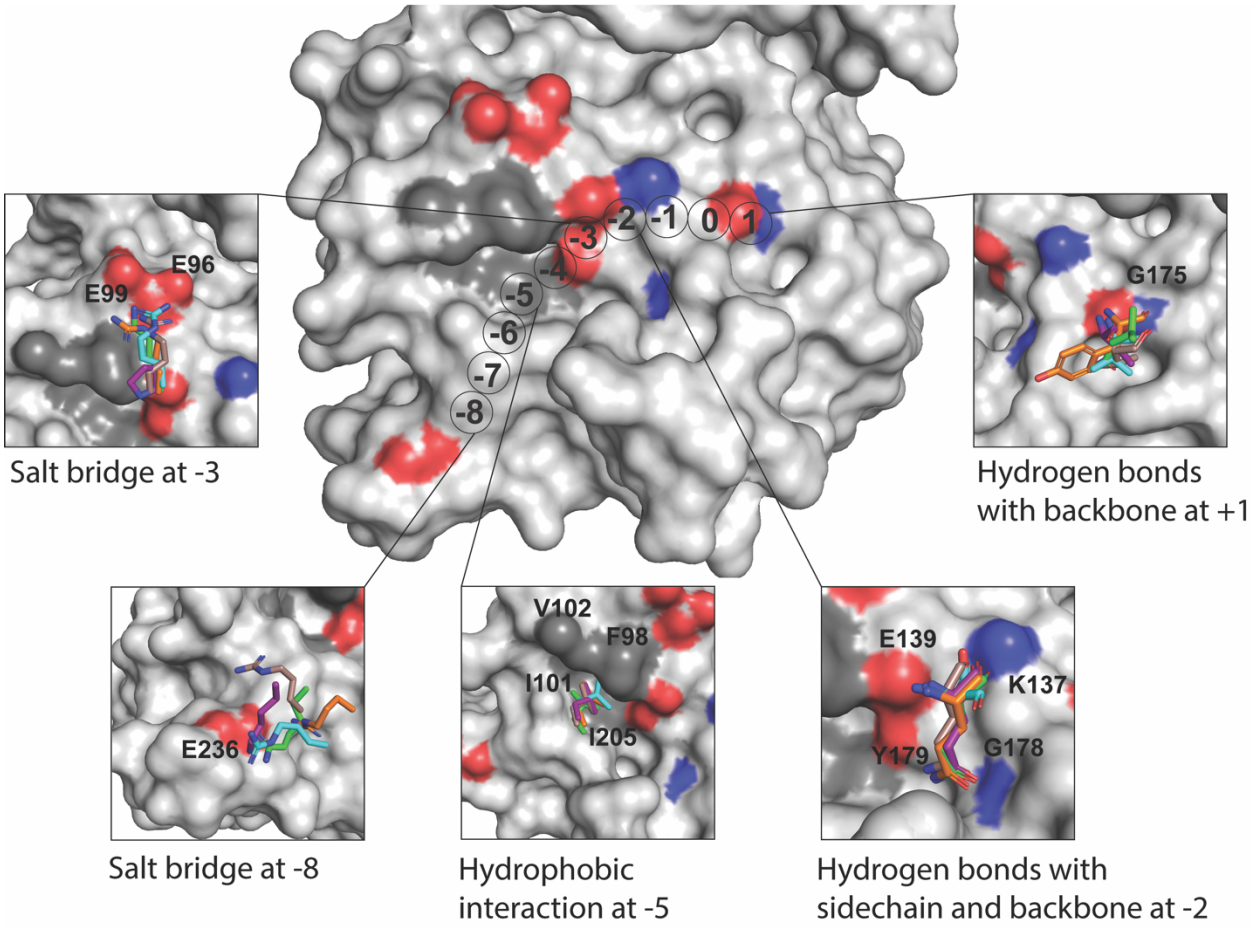

Figure 3. Conserved binding motifs on the catalytic domain surface.
Surface representation of the CaMKII kinase domain highlighting residues shown to interact with binding partners.

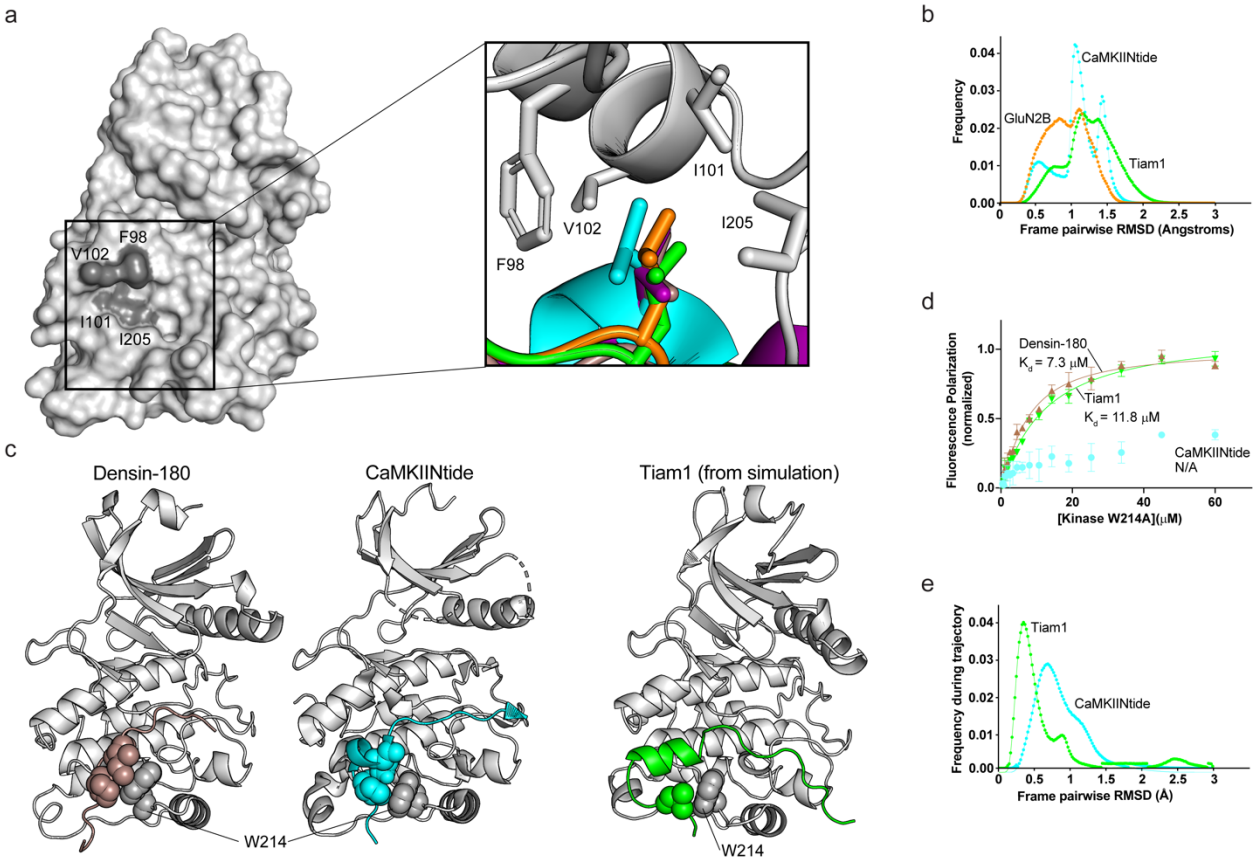

Figure 4. Hydrophobic interactions mediate binding. (a) Surface representation of CaMKII kinase domain with residues forming the hydrophobic pocket labeled. Zoom in: Overlay of leucine residues from all co-crystal structures bound in the hydrophobic pocket. (b) Histograms of RMSD between every pair of trajectory frames for F98, I101, V102, and I205 with -5 peptide leucine. (c) Sphere representation of the isoleucine and proline or leucine residue of Densin-180 (brown), CaMKIIN (cyan), and Tiam1 (green) docking onto W214 (gray) of kinase domain. (d) FP measurements of the CaMKII kinase domain with W214A mutation binding to CaMKIIN (cyan), Densin-180 (brown), and Tiam1 (green) peptides. (e) RMSD histograms for W214 interacting with isoleucine and proline of CaMKIIN1 and leucine of Tiam1 as seen in 3c.

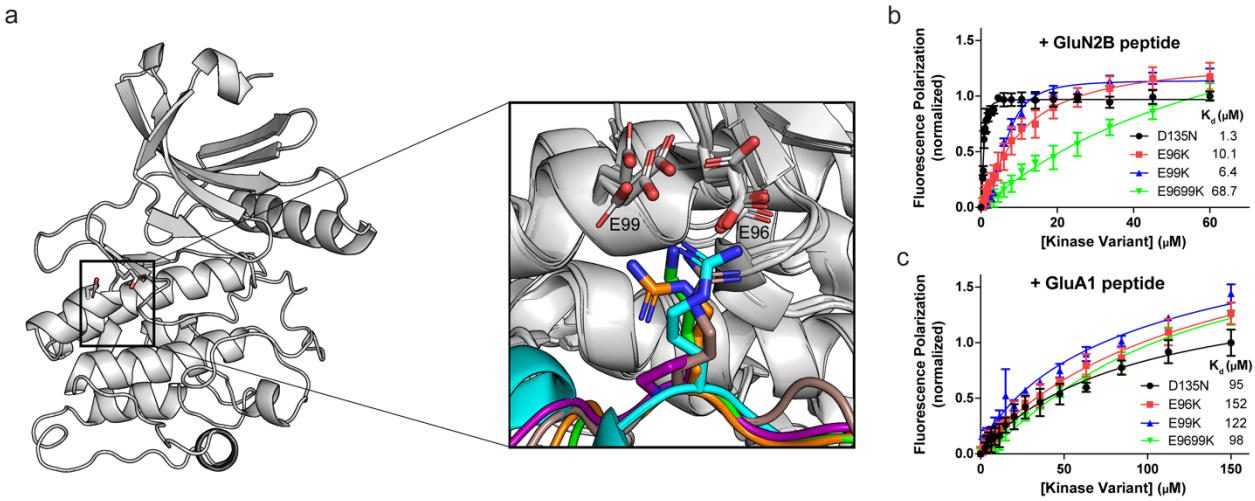

Figure 5. Electrostatic interactions with E96 and E99 facilitate high affinity binding. (a) CaMKII kinase domain shown as a cartoon, E96 and E99 residues are shown in sticks. Inset: zoom in of all five co-crystal structures overlaid. (b) FP measurements of the CaMKII kinase domain with E96K (red), E99K (blue), and E9699K (green) mutations binding to the GluN2B peptide and (c) to the GluA1 peptide.

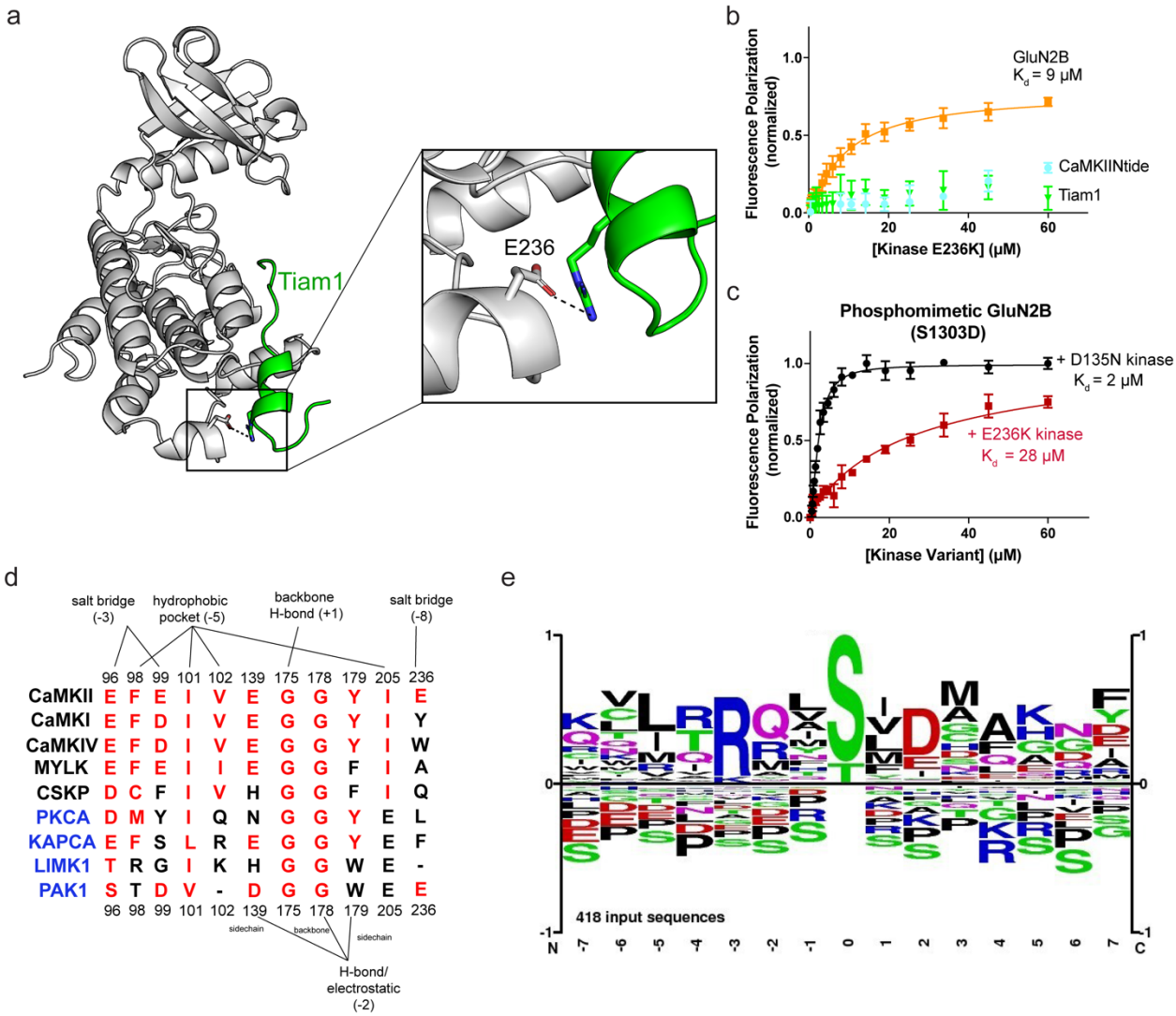

Figure 6. Electrostatic interaction with E236 has distinctive effects on binding. (a) View of the interaction between CaMKII E236 residue (gray) and Tiam1 R1549 residue (green). (b) FP measurements of the CaMKII kinase domain with E236K mutation binding to GluN2B (orange), CaMKIIN (cyan), and Tiam1 (green) peptides. (c) FP measurements of the phosphomimetic GluN2B peptide (S1303D) binding to either WT CaMKII kinase domain (D135N, black) or mutant kinase domain (E236K, magenta). (d) Alignment of key residues involved in binding substrates across kinases from the Ca^{2+}/CaM family (black text) and four kinases from different families (blue text). PKCA and KAPCA (cAMP dependent kinase) belong to the AGC Ser/Thr family. LimK1 and Pak1 belong to TKL and STE Ser/Thr family. (e) The sequence logo for all previously identified substrates of CaMKII from the PhosphoSitePlus database with the phosphorylation site at the 0 position.

612 **REFERENCES**
613

614 1. Lisman, J., R. Yasuda, and S. Raghavachari, *Mechanisms of CaMKII action in long-term*
615 *potentiation.* Nat Rev Neurosci, 2012. **13**(3): p. 169-82.
616 2. Malenka, R.C., et al., *An essential role for postsynaptic calmodulin and protein kinase*
617 *activity in long-term potentiation.* Nature, 1989. **340**(6234): p. 554-7.
618 3. Sloutsky, R. and M.M. Stratton, *Functional implications of CaMKII alternative splicing.*
619 Eur J Neurosci, 2020.
620 4. Erondu, N.E. and M.B. Kennedy, *Regional distribution of type II Ca2+/calmodulin-*
621 *dependent protein kinase in rat brain.* J Neurosci, 1985. **5**(12): p. 3270-7.
622 5. Omkumar, R.V., et al., *Identification of a phosphorylation site for*
623 *calcium/calmodulindependent protein kinase II in the NR2B subunit of the N-methyl-D-*
624 *aspartate receptor.* J Biol Chem, 1996. **271**(49): p. 31670-8.
625 6. Mammen, A.L., et al., *Phosphorylation of the alpha-amino-3-hydroxy-5-*
626 *methylisoxazole4-propionic acid receptor GluR1 subunit by calcium/calmodulin-*
627 *dependent kinase II.* J Biol Chem, 1997. **272**(51): p. 32528-33.
628 7. Barria, A., V. Derkach, and T. Soderling, *Identification of the Ca2+/calmodulin-dependent*
629 *protein kinase II regulatory phosphorylation site in the alpha-amino-3-hydroxyl-5-*
630 *methyl-4-isoxazole-propionate-type glutamate receptor.* J Biol Chem, 1997. **272**(52): p.
631 32727-30.
632 8. Ishida, A. and H. Fujisawa, *Stabilization of Calmodulin-Dependent Protein-Kinase-Ii*
633 *through the Autoinhibitory Domain.* Journal of Biological Chemistry, 1995. **270**(5): p.
634 2163-2170.
635 9. Bayer, K.U., et al., *Interaction with the NMDA receptor locks CaMKII in an active*
636 *conformation.* Nature, 2001. **411**(6839): p. 801-5.
637 10. Bayer, K.U., et al., *Transition from reversible to persistent binding of CaMKII to*
638 *postsynaptic sites and NR2B.* J Neurosci, 2006. **26**(4): p. 1164-74.
639 11. Saneyoshi, T., et al., *Reciprocal Activation within a Kinase-Effector Complex Underlying*
640 *Persistence of Structural LTP.* Neuron, 2019. **102**(6): p. 1199-1210 e6.
641 12. Walikonis, R.S., et al., *Densin-180 forms a ternary complex with the (alpha)-subunit of*
642 *Ca2+/calmodulin-dependent protein kinase II and (alpha)-actinin.* J Neurosci, 2001.
643 **21**(2): p. 423-33.
644 13. Jiao, Y., et al., *Characterization of a central Ca2+/calmodulin-dependent protein kinase*
645 *IIalpha/beta binding domain in densin that selectively modulates glutamate receptor*
646 *subunit phosphorylation.* J Biol Chem, 2011. **286**(28): p. 24806-18.
647 14. Diering, G.H. and R.L. Huganir, *The AMPA Receptor Code of Synaptic Plasticity.* Neuron,
648 2018. **100**(2): p. 314-329.
649 15. Barria, A., et al., *Regulatory phosphorylation of AMPA-type glutamate receptors by CaM-*
650 *KII during long-term potentiation.* Science, 1997. **276**(5321): p. 2042-5.
651 16. Derkach, V., A. Barria, and T.R. Soderling, *Ca2+/calmodulin-kinase II enhances channel*
652 *conductance of alpha-amino-3-hydroxy-5-methyl-4-isoxazolepropionate type glutamate*
653 *receptors.* Proc Natl Acad Sci U S A, 1999. **96**(6): p. 3269-74.
654 17. Chao, L.H., et al., *Intersubunit capture of regulatory segments is a component of*
655 *cooperative CaMKII activation.* Nat Struct Mol Biol, 2010. **17**(3): p. 264-72.

656 18. Castro-Rodrigues, A.F., et al., *The Interaction between the Drosophila EAG Potassium*
657 *Channel and the Protein Kinase CaMKII Involves an Extensive Interface at the Active Site*
658 *of the Kinase.* J Mol Biol, 2018. **430**(24): p. 5029-5049.
659 19. Wang, C., et al., *A novel endogenous human CaMKII inhibitory protein suppresses tumor*
660 *growth by inducing cell cycle arrest via p27 stabilization.* J Biol Chem, 2008. **283**(17): p.
661 11565-74.
662 20. Zhang, J., et al., *Molecular cloning and characterization of a novel calcium/calmodulin-*
663 *dependent protein kinase II inhibitor from human dendritic cells.* Biochem Biophys Res
664 Commun, 2001. **285**(2): p. 229-34.
665 21. Chang, B.H., S. Mukherji, and T.R. Soderling, *Calcium/calmodulin-dependent protein*
666 *kinase II inhibitor protein: localization of isoforms in rat brain.* Neuroscience, 2001.
667 **102**(4): p. 767-77.
668 22. White, R.R., et al., *Definition of optimal substrate recognition motifs of Ca2+-calmodulin-*
669 *dependent protein kinases IV and II reveals shared and distinctive features.* J Biol Chem,
670 1998. **273**(6): p. 3166-72.
671 23. Songyang, Z., et al., *A structural basis for substrate specificities of protein Ser/Thr*
672 *kinases: primary sequence preference of casein kinases I and II, NIMA, phosphorylase*
673 *kinase, calmodulin-dependent kinase II, CDK5, and Erk1.* Mol Cell Biol, 1996. **16**(11): p.
674 6486-93.
675 24. Ishida, A., et al., *Critical amino acid residues of AIP, a highly specific inhibitory peptide of*
676 *calmodulin-dependent protein kinase II.* FEBS Lett, 1998. **427**(1): p. 115-8.
677 25. Stokoe, D., et al., *The substrate specificity and structure of mitogen-activated protein*
678 *(MAP) kinase-activated protein kinase-2.* Biochem J, 1993. **296 (Pt 3)**: p. 843-9.
679 26. Coultrap, S.J. and K.U. Bayer, *Improving a natural CaMKII inhibitor by random and*
680 *rational design.* PLoS One, 2011. **6**(10): p. e25245.
681 27. Yang, E. and H. Schulman, *Structural examination of autoregulation of multifunctional*
682 *calcium/calmodulin-dependent protein kinase II.* J Biol Chem, 1999. **274**(37): p. 26199-
683 208.
684 28. Rellos, P., et al., *Structure of the CaMKIIdelta/calmodulin complex reveals the molecular*
685 *mechanism of CaMKII kinase activation.* PLoS Biol, 2010. **8**(7): p. e1000426.
686 29. Rust, H.L. and P.R. Thompson, *Kinase consensus sequences: a breeding ground for*
687 *crosstalk.* ACS Chem Biol, 2011. **6**(9): p. 881-92.
688 30. Zha, M., et al., *Crystal structures of human CaMKIalpha reveal insights into the*
689 *regulation mechanism of CaMKI.* PLoS One, 2012. **7**(9): p. e44828.
690 31. Mao, L.M., et al., *Phosphorylation and regulation of glutamate receptors by CaMKII.*
691 Sheng Li Xue Bao, 2014. **66**(3): p. 365-72.
692 32. Halt, A.R., et al., *CaMKII binding to GluN2B is critical during memory consolidation.*
693 EMBO J, 2012. **31**(5): p. 1203-16.
694 33. Hosokawa, T., et al., *Stoichiometry and phosphoisotypes of hippocampal AMPA-type*
695 *glutamate receptor phosphorylation.* Neuron, 2015. **85**(1): p. 60-67.
696 34. Diering, G.H., et al., *Extensive phosphorylation of AMPA receptors in neurons.* Proc Natl
697 Acad Sci U S A, 2016. **113**(33): p. E4920-7.
698 35. Kury, S., et al., *De Novo Mutations in Protein Kinase Genes CAMK2A and CAMK2B Cause*
699 *Intellectual Disability.* Am J Hum Genet, 2017. **101**(5): p. 768-788.

700 36. Torres-Ocampo, A.P., et al., *Characterization of CaMKII alpha holoenzyme stability.*
701 Protein Science, 2020.
702 37. McCoy, F., et al., *Metabolic activation of CaMKII by coenzyme A.* Mol Cell, 2013. **52**(3): p.
703 325-39.
704 38. Wang, X., et al., *A novel mechanism for Ca(2+)/calmodulin-dependent protein kinase II*
705 *targeting to L-type Ca(2+) channels that initiates long-range signaling to the nucleus.* J
706 Biol Chem, 2017. **292**(42): p. 17324-17336.
707 39. McCoy, A.J., et al., *Phaser crystallographic software.* J Appl Crystallogr, 2007. **40**(Pt 4): p.
708 658-674.
709 40. Murshudov, G.N., A.A. Vagin, and E.J. Dodson, *Refinement of macromolecular structures*
710 *by the maximum-likelihood method.* Acta Crystallogr D Biol Crystallogr, 1997. **53**(Pt 3): p.
711 240-55.
712 41. Winn, M.D., et al., *Overview of the CCP4 suite and current developments.* Acta
713 Crystallogr D Biol Crystallogr, 2011. **67**(Pt 4): p. 235-42.
714 42. Eastman, P., et al., *OpenMM 4: A Reusable, Extensible, Hardware Independent Library*
715 *for High Performance Molecular Simulation.* J Chem Theory Comput, 2013. **9**(1): p. 461-
716 469.
717 43. Pall, S., et al., *Tackling Exascale Software Challenges in Molecular Dynamics Simulations*
718 *with GROMACS.* Solving Software Challenges for Exascale, 2015. **8759**: p. 3-27.
719 44. Huang, J., et al., *CHARMM36m: an improved force field for folded and intrinsically*
720 *disordered proteins.* Nat Methods, 2017. **14**(1): p. 71-73.
721 45. Jorgensen, W.L., et al., *Comparison of Simple Potential Functions for Simulating Liquid*
722 *Water.* Journal of Chemical Physics, 1983. **79**(2): p. 926-935.
723 46. Hess, B., *P-LINCS: A Parallel Linear Constraint Solver for Molecular Simulation.* J Chem
724 Theory Comput, 2008. **4**(1): p. 116-22.
725 47. Feenstra, K.A., B. Hess, and H.J.C. Berendsen, *Improving efficiency of large time-scale*
726 *molecular dynamics simulations of hydrogen-rich systems.* Journal of Computational
727 Chemistry, 1999. **20**(8): p. 786-798.
728 48. Essmann, U., et al., *A Smooth Particle Mesh Ewald Method.* Journal of Chemical Physics,
729 1995. **103**(19): p. 8577-8593.
730 49. Bussi, G., D. Donadio, and M. Parrinello, *Canonical sampling through velocity rescaling.* J
731 Chem Phys, 2007. **126**(1): p. 014101.
732 50. Parrinello, M. and A. Rahman, *Polymorphic Transitions in Single-Crystals - a New*
733 *Molecular-Dynamics Method.* Journal of Applied Physics, 1981. **52**(12): p. 7182-7190.
734 51. Larsson, P., R.C. Kneiszl, and E.G. Marklund, *MkVsites: A tool for creating GROMACS*
735 *virtual sites parameters to increase performance in all-atom molecular dynamics*
736 *simulations.* J Comput Chem, 2020. **41**(16): p. 1564-1569.
737 52. McGibbon, R.T., et al., *MDTraj: A Modern Open Library for the Analysis of Molecular*
738 *Dynamics Trajectories.* Biophys J, 2015. **109**(8): p. 1528-32.
739